

A Low-Complexity Post-Weighting Predistorter in a mMIMO Transmitter Under Crosstalk

Ganesh Prasad, *Member, IEEE* and Håkan Johansson, *Senior Member, IEEE*

Abstract—In hybrid beamforming, the beam oriented digital predistortion (BO-DPD) is incompetent to linearize the output in different directions except the desired direction to the transmitter. Therefore, subsequent to the BO-DPD operation, we perform a post-weighting (PW) processing to minimize the nonlinear radiations in the wide range of directions. Here, the optimized PW coefficients are multiplied by the polynomial basis functions of the BO-DPD, then, the resultant signals are distributed to the PAs to compensate the nonlinear radiations. In this work, first, we propose fully-featured post-weighting (FF-PW) scheme, then, we derive a low-complexity post-weighting (LC-PW) scheme.

Index Terms—Predistortion, polynomial model, hybrid beamforming, post-weighting, convex optimization

I. INTRODUCTION

For efficient transmission of signals, radio frequency (RF) power amplifiers (PAs) play an important role. However, the design of highly linear PAs over the large dynamic range of the signals like orthogonal frequency-division multiplexing (OFDM) with high peak-to-average power ratio is expensive. Further, it is not economical for a massive multiple-input multiple-output (mMIMO) transmitter with a large number of PAs. Besides, a single digital predistortion (DPD) is incompetent to deal with the nonlinearities of more than one PAs with different nonlinear characteristics that needs to be addressed. In this work, we aim to minimize the nonlinear output radiation of a beam-oriented (BO) subarray in presence of crosstalk.

The authors in [1] proposed algorithms to mitigate the nonlinear effect of crosstalk before the PAs. In [2], the crosstalk is estimated and accordingly the DPD is trained to alleviate its effect at the output of hybrid beamforming. However, these works have not investigated the BO nonlinear output from an array of PAs. In this regard, a beam oriented DPD (BO-DPD)¹ learning algorithm has been proposed in [3], but, it performs the linearization in a particular direction. In [4], a full-angle DPD is designed to provide the linearization in different directions. First, it compensates the differences among the PAs using a tuning box followed by the linearization. Nevertheless, as evident in [5], a single DPD is incompetent to linearize the array of PAs. To address it, two post-weighting (PW) schemes that work after the training of the DPD are described in [6] in the absence of the crosstalk signals. However, in that work, for a given PA of the subarray, one PW coefficient is applied along all the basis functions of a general polynomial model (GMP) of the DPD. Thus, due to a less degree of freedom, it is unable to linearize the output radiation in a wide range of directions.

Besides, in its intra PW scheme, the required number of radio frequency (RF) chains is same as the total number of PAs which is not economical for a mMIMO transmitter.

In general, the fundamental behind the linearization of a mMIMO transmitter is described as follows. Practically, the S PAs in a subarray have different nonlinear characteristics. Typically, a DPD takes almost same set of Q basis functions with respective Q nonzero coefficients to linearize a PA of the subarray. Therefore, ideally, S DPDs are required with total $S \times Q$ coefficients to get desired output. But, it makes the mMIMO transmitter complex and costly. Therefore, the existing works use a single DPD with Q coefficients (S times less than the ideal case) to linearize the BO output from the S PAs. But, it is less capable to linearize in other directions because of not linearizing all the PAs. In this work, we address it using a novel low-complexity PW (LC-PW) scheme, derived from a fully-featured (FF) PW (FF-PW) that operates after the training of the single DPD.

The key contribution of this work is three-fold as follows. (i) First, we express the polynomial models for the DPD and PAs in their matrix forms. Then, the crosstalk over the PAs are approximated for the BO transmitter with beamforming weights. Afterwards, we train the DPD for the BO output. (ii) Next, we propose a FF-PW scheme and describe the challenges to implement it. Using that we derive an architecture for LC-PW scheme. Based on the architecture, the system parameters are arranged non-trivially into suitable vectors and matrices to simplify the system analysis. (iii) Further, an expression for nonlinear radiation is obtained for the BO transmitter operating with DPD and PW. Considering its sum of average power in a discrete range of directions as an objective function, a convex minimization problem is formulated. Its optimal solution is obtained using Karush–Kuhn–Tucker (KKT) conditions. Finally, numerical results are obtained to get various design insights.

II. SYSTEM DESCRIPTION AND BO-DPD TRAINING

Fig. 1 represents a subarray of a mMIMO transmitter with hybrid beamforming. The transmitter operates with BO-DPD and PW architecture to compensate nonlinear radiation in the presence of crosstalk signals. Here, similar to typical linearization of PAs [7], first, the DPD is trained. Then, the output of the trained DPD is inputted to the PW block for further linearization. Thereafter, we get the desired linear output from the PAs. Next, we describe the system parameters and training process of the DPD, however, the PW architecture parameters are described in Section III.

A. System Representation

In the mMIMO transmitter, we consider a uniform linear array of $K \times S$ PAs where each of K subarrays contains S

G. Prasad and H. Johansson are with the Division of Communication Systems, Department of Electrical Engineering, Linköping University, 581 83 Linköping, Sweden (e-mail: {ganesh.prasad, hakan.johansson}@liu.se).

¹In this work, the terms DPD and BO-DPD are used interchangeably.

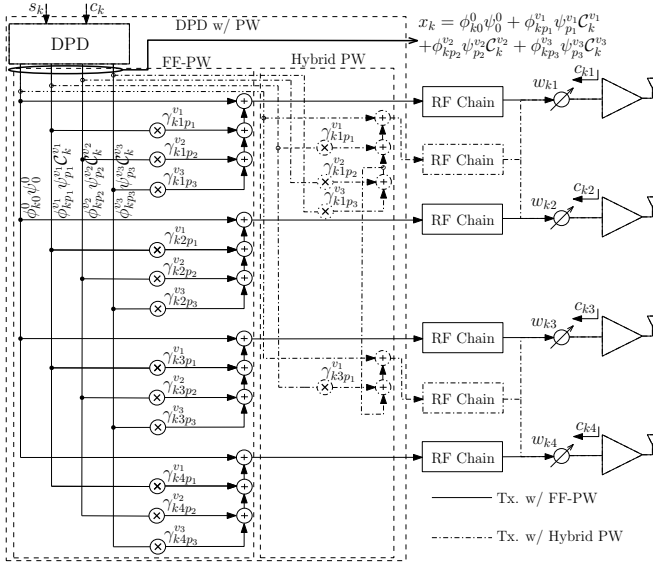


Fig. 1. Post-weighting (PW) digital predistortion architecture.

PAs. For instance, Fig. 1 represents $S = 4$ PAs in the k th subarray. The inputs to the DPD are the baseband message signal s_k and the estimated crosstalk signal c_k . The vector of message signals is denoted as $\mathbf{s} = [s_1, \dots, s_K]^T$. We consider the dual-input memoryless polynomial models² [7] for the predistorter and nonlinear output signals from the DPD and PAs in presence of the crosstalk signals. After omitting the nonlinear terms of the crosstalk signal c_k , the output x_k of the DPD in k th subarray can be expressed in (1a) which is further represented in matrix form in (1b).

$$x_k = \sum_{p=0}^{(P-1)/2} \phi_{kp}^0 \psi_p^0(s_k) + \sum_{p=0}^{(P-1)/2} \phi_{kp}^1 \psi_p^1(s_k) c_k + \sum_{p=1}^{(P-1)/2} \phi_{kp}^2 \psi_p^2(s_k) c_k^*, \quad (1a)$$

$$x_k = \Psi(s_k, c_k) \Phi_k; \quad k \in \{1, 2, \dots, K\}, \quad (1b)$$

where P is the order of the polynomial³ and $\Psi(s_k, c_k) = [\Psi^0(s_k), \Psi^1(s_k) c_k, \Psi^2(s_k) c_k^*]$, $\Psi^v(s_k) = [\psi_{\mu}^v(s_k), \dots, \psi_{(P-1)/2}^v(s_k)]$ for $v \in \{0, 1, 2\}$. $\psi_p^0(s_k) = s_k^{p+1} s_k^{*p}$, $\psi_p^1(s_k) = s_k^p s_k^{*p}$, and $\psi_p^2(s_k) = s_k^{p+1} s_k^{*p-1}$ are the basis functions. μ is the initial value of p and $\mu = 1$ for $v = 2$; otherwise, $\mu = 0$. Φ_k is a column vector of the coefficients for the basis functions in $\Psi(s_k, c_k)$, given by $\Phi_k = [\Phi_k^0, \Phi_k^1, \Phi_k^2]^T$. $\Phi_k^v = [\phi_{k\mu}^v, \dots, \phi_{k(P-1)/2}^v]^T$ and ϕ_{kp}^v is the coefficient of basis $\psi_p^v(s_k)$. Moreover, output signal vector of K DPDs is denoted as $\mathbf{x} = [x_1, \dots, x_K]^T$. Similarly, for the inputs, x_k and c_{kl} (the crosstalk signal) to the l th PA of the k th subarray, its output y_{kl} is expressed using the dual-input memoryless model as in (2a) and its matrix form in (2b).

$$y_{kl} = \sum_{p=0}^{(P-1)/2} \phi_{klp}^0 \psi_p^0(w_{kl} x_k) + \sum_{p=0}^{(P-1)/2} \phi_{klp}^1 \psi_p^1(w_{kl} x_k) c_{kl} + \sum_{p=1}^{(P-1)/2} \phi_{klp}^2 \psi_p^2(w_{kl} x_k) c_{kl}^* \quad (2a)$$

$$y_{kl} = \Psi(w_{kl} x_k, c_{kl}) \Phi_{kl}; \quad l \in \{1, 2, \dots, S\}, \quad (2b)$$

²For simplicity, we consider the memoryless polynomial models, however, the proposed work is equally applicable for memory polynomial models.

³Although, for simplicity, the orders of the polynomials are represented by same symbol, P in (1a) and (2a), but, they can take different values.

where $\Psi(w_{kl} x_k, c_{kl})$ and Φ_{kl} are the row and column vectors of the basis functions and its coefficients respectively. They can be represented similarly as described above for the DPD basis functions and coefficients with additional suffix l to represent it for l th PA of the subarray. Note that the PAs coefficients Φ_{kl} ; $l \in \{1, \dots, S\}$ are assumed to be known which can be identified using least square (LS) estimation as described briefly in the numerical section. w_{kl} ($|w_{kl}| = 1$) is the beamforming weight to the l th PA of the k th subarray. Moreover, the beamforming vector of k th subarray is $\mathbf{w}_k = [w_{k1}, \dots, w_{kS}]^T$. Further, all the outputs from the PAs can be expressed in a matrix form as:

$$\mathbf{Y}_k = \Omega_k \Theta_k, \quad (3)$$

where $\mathbf{Y}_k = [y_{k1}, \dots, y_{kS}]^T$, $\Omega_k = \text{diag}([\Psi(w_{k1} x_k, c_{k1})^T, \dots, \Psi(w_{kS} x_k, c_{kS})^T]^T)$ and $\Theta_k = [\Phi_{k1}^T, \dots, \Phi_{kS}^T]^T$.

Now, we represent the output radiation from the subarray in a particular direction and crosstalk signals associated with PAs as follows. For the steering vector \mathbf{h}_k^φ at angle φ to the vertical plane of the array, the BO signal to the direction (angle) is:

$$z_k^\varphi = \mathbf{h}_k^\varphi T \mathbf{Y}_k = \mathbf{h}_k^\varphi T \Omega_k \Theta_k, \quad (4)$$

where $\mathbf{h}_k^\varphi = [h_{k1}^\varphi, \dots, h_{kS}^\varphi]^T$ and h_{kl}^φ is the l th steering element. As the crosstalk signal c_{kl} cannot be measured at the l th PA, to determine it, we assume that the crosstalk signal at a PA of a subarray is due to linear combination of the transmit signals from the other PAs [2]. Thus, c_{kl} can be expressed as:

$$c_{kl} = \sum_{i=1}^K \sum_{r=1}^S \lambda'_{kl,ir} y_{ir} = \lambda'_{kl} \mathbf{Y}, \quad (5)$$

where $\lambda'_{kl} = [\lambda'_{kl,1}, \dots, \lambda'_{kl,K}]$, and $\lambda'_{kl,i} = [\lambda'_{kl,i1}, \dots, \lambda'_{kl,iS}]$, and $\mathbf{Y} = [\mathbf{Y}_1^T, \dots, \mathbf{Y}_K^T]^T$. $\lambda'_{kl,ir}$ is the coefficient for contribution in crosstalk signal c_{kl} at l th PA of the k th subarray from r th PA of the i th subarray. Simplifying (5) in linear terms of c_{ir} and DPD output x_k after omitting the negligible nonlinear terms, we get c_{kl} as in (6a). Using it, all crosstalk signals in matrix form can be obtained in (6b) which is further simplified in (6c).

$$c_{kl} = \sum_{i=1}^K \sum_{r=1}^S [\lambda'_{kl,ir} \phi_{ir0}^0 w_{ir} x_i + \lambda'_{kl,ir} \phi_{ir0}^1 c_{ir}] \quad (6a)$$

$$\mathbf{c} = \mathbf{A}^0 \mathbf{W}_D \mathbf{x} + \mathbf{A}^1 \mathbf{c} \quad (6b)$$

$$\Rightarrow \mathbf{c} = (\mathbf{I} - \mathbf{A}^1)^{-1} \mathbf{A}^0 \mathbf{W}_D \mathbf{x} = \Lambda \mathbf{W}_D \mathbf{x}, \quad (6c)$$

where $\mathbf{c} = [\bar{c}_1^T, \dots, \bar{c}_K^T]^T$, $\bar{c}_k = [c_{k1}, \dots, c_{kS}]^T$, $\mathbf{A}^v = \bar{\Lambda} \text{diag}(\bar{\Phi}_1^v, \dots, \bar{\Phi}_K^v)$, $\bar{\Phi}_k^v = [\phi_{k10}^v, \dots, \phi_{kS0}^v]$ for $v \in \{0, 1\}$, $\bar{\Lambda} = [\lambda_{11}^T, \dots, \lambda_{1S}^T, \dots, \lambda_{K1}^T, \dots, \lambda_{KS}^T]^T$, and $\mathbf{W}_D = \text{diag}([w_{11}, \dots, w_{1S}]^T, \dots, [w_{K1}, \dots, w_{KS}]^T)$. From (6c), it is evident that $\Lambda = (\mathbf{I} - \mathbf{A}^1)^{-1} \mathbf{A}^0$ which is nothing but the coefficients associated with the weighted signal vector $\mathbf{W}_D \mathbf{x}$ to get the crosstalk signal vector, \mathbf{c} . It can be expressed as $\Lambda = [\Lambda_1^T, \dots, \Lambda_K^T]^T$, where $\Lambda_k = [\lambda_{k1}^T, \dots, \lambda_{kS}^T]^T$ and $\lambda_{kl} = [\lambda_{kl,11}, \dots, \lambda_{kl,1S}, \dots, \lambda_{kl,K1}, \dots, \lambda_{kl,KS}]$. Next, using the above representations of BO output signal in (4) and the crosstalk in (6c), we describe the training of BO-DPD.

B. Training of BO-DPD

Here, first, we determine the crosstalk signals \bar{c}_k to the PAs as a function of crosstalk input c_k to the DPD. As c_k depends on the crosstalk coefficients which are represented as a function of measured BO output z_k^φ . Then, using these

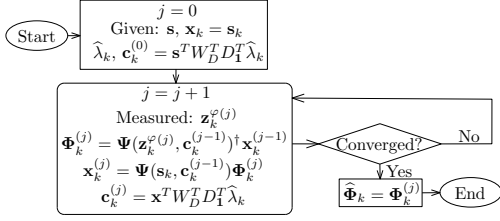


Fig. 2. Flow diagrams for the identification of DPD coefficients.

relationships, the DPD coefficients Φ_k are determined using the algorithm as shown in Fig. 2.

In [2], the relationship between c_k and \bar{c}_k is established without considering beamforming weights w_k . To establish it with w_k , first, we consider the same approximation, $\lambda_{kl,ir} \approx \alpha_l \lambda_{ki}$ due to uniform and linear arrangement of PAs [2]. It denotes that the crosstalk from r th PA of the i th subarray to l th PA of the k th subarray with coefficient $\lambda_{kl,ir}$ can be approximated to α_l times the overall crosstalk from the i th subarray to k th subarray with coefficient λ_{ki} . After applying the approximation to λ_{kl} (cf. Section II-A), it is expressed as: $\lambda_{kl} \approx \alpha_l [\lambda_{k1}, \dots, \lambda_{k1}, \dots, \lambda_{kK}, \dots, \lambda_{kK}] =$

$$\alpha_l [\lambda_{k1} \mathbf{1}_S^T, \dots, \lambda_{kK} \mathbf{1}_S^T] = \alpha_l \lambda_k^T D_1, \text{ where } \lambda_k = [\lambda_{k1}, \dots, \lambda_{kK}]^T, D_1 = \text{diag}(\underbrace{\mathbf{1}_S^T}_{S \text{ times}}, \dots, \underbrace{\mathbf{1}_S^T}_{S \text{ times}})$$

the column vector of ones of length S . Thus, Λ_k (cf. Section II-A) is: $\Lambda_k \approx \alpha \lambda_k^T D_1$, where $\alpha = [\alpha_1, \dots, \alpha_S]^T$. After applying this approximation in (6c), we get:

$$\bar{c}_k = \alpha c_k, \quad (7)$$

where $c_k = \mathbf{x}^T W_D^T D_1^T \lambda_k$ is the estimate of the crosstalk at the input to the DPD of the k th subarray. Using (7), the inputs to the basis functions in Ω_k of (3) can be expressed in x_k and c_k . As c_k depends on λ_k , we estimate λ_k to find c_k . In this regard, for the given input x_k to the PAs and the measured BO output z_k^φ , the coefficients λ_k are estimated as follows. First, by expanding, z_k^φ in (4) can be expressed as:

$$z_k^\varphi = g_k^0 + g_k^1 \hat{\lambda}_k + g_k^2 \hat{\lambda}_k^*, \quad (8)$$

where $g_k^0 = \sum_{l=1}^S h_{kl}^\varphi \Psi^0(w_{kl} x_k) \hat{\Phi}_{kl}^0$, $g_k^1 = \sum_{l=1}^S h_{kl}^\varphi \Psi^1(w_{kl} x_k) \hat{\Phi}_{kl}^1 \mathbf{x}^T W_D^T D_1^T$, and $g_k^2 = \sum_{l=1}^S h_{kl}^\varphi \Psi^2(w_{kl} x_k) \hat{\Phi}_{kl}^2 \mathbf{x}^H W_D^H D_1^H$. Further, (8) can be extended by including the time samples of \mathbf{x} where the time dependent variables, z_k^φ , g_k^0 , g_k^1 , and g_k^2 are denoted as z_k^φ , \mathbf{g}_k^0 , \mathbf{G}_k^1 , and \mathbf{G}_k^2 , respectively. Thus, z_k^φ can be expressed as:

$$z_k^\varphi = \mathbf{g}_k^0 + \mathbf{G}_k^1 \hat{\lambda}_k + \mathbf{G}_k^2 \hat{\lambda}_k^*. \quad (9)$$

By splitting (9) into real and imaginary parts, the real part, $\mathcal{R}(\hat{\lambda}_k)$ and imaginary part, $\mathcal{I}(\hat{\lambda}_k)$, can be determined as:

$$\begin{bmatrix} \mathcal{R}(\hat{\lambda}_k) \\ \mathcal{I}(\hat{\lambda}_k) \end{bmatrix} = \begin{bmatrix} \mathcal{R}(\mathbf{G}_k^1 + \mathbf{G}_k^2) & \mathcal{I}(-\mathbf{G}_k^1 + \mathbf{G}_k^2) \\ \mathcal{I}(\mathbf{G}_k^1 + \mathbf{G}_k^2) & \mathcal{R}(\mathbf{G}_k^1 - \mathbf{G}_k^2) \end{bmatrix}^{-1} \begin{bmatrix} \mathcal{R}(z_k^\varphi - \mathbf{g}_k^0) \\ \mathcal{I}(z_k^\varphi - \mathbf{g}_k^0) \end{bmatrix} \quad (10)$$

Using (10), the coefficients of the DPD are trained using the algorithm as shown in Fig. 2. Here, initially, the output of the DPD is set as $\mathbf{x}_k = s_k$ and corresponding crosstalk c_k is determined. Then, in the following step, the measured output signal, z_k^φ is set as another input to the DPD to determine its coefficients Φ_k using LS method. Using it, the output \mathbf{x}_k

of the DPD and c_k are computed. The process repeats until the value of Φ_k converges. Note that while the training, the closed loop feedback from the output of the PAs to the DPD as described in [6, cf. Fig. 2] is not shown in Fig. 1 for simplicity.

III. POST-WEIGHTING SCHEMES AND OPTIMIZATION

In the PW block as shown in Fig. 1, the input is the output from the trained BO-DPD, and the output of the block is inputted to the PAs. In this section, we describe two PW schemes and their optimizations. Here, first, we express z_k^φ in terms of message signal s_k by substituting (1b) into (8). Separating the first basis function from the rest, we get:

$$z_k^\varphi = \mathbf{h}_k^{\varphi T} \mathbf{W}_k \tilde{\Phi}_{k0}^0 \phi_{k0}^0 s_k + \mathbf{h}_{k0}^{\varphi T} \mathbf{W}_k \tilde{\Phi}_{k0}^0 \Psi'(s_k, c_k) \Phi_k' + Z_{k,NL}^\varphi \quad (11)$$

where $\mathbf{W}_k = \text{diag}(\mathbf{w}_k)$, $\tilde{\Phi}_{k0}^0 = [\phi_{k10}^0, \dots, \phi_{kS0}^0]^T$, $\Psi'(s_k, c_k) = \{\Psi(s_k, c_k) \setminus \psi_0^0(s_k) = s_k\}$, $\Phi_k' = \{\Phi_k \setminus \phi_{k0}^0\}$, and $Z_{k,NL}$ is the nonlinear higher order terms, obtained after removing the term consisting first (linear) basis function in (4). In (11), the first term is the desired output of the subarray, but the second and third terms inject nonlinearities in the radiation, thus, the nonlinear radiation $z_{k,NL}^\varphi$ can be expressed as:

$$z_{k,NL}^\varphi = \mathbf{h}_k^{\varphi T} \mathbf{W}_k \tilde{\Phi}_{k0}^0 \Psi'(s_k, c_k) \Phi_k' + Z_{k,NL}^\varphi. \quad (12)$$

In (12), $z_{k,NL}^\varphi$ gives the nonlinearities in azimuth directions to the mMIMO transmitter, except angle φ . Because, in BO-DPD, its coefficients Φ_k' are trained to provide the linearization in the direction φ . Therefore, we adopt the PW schemes to reduce the nonlinear power radiation in the directions other than φ . Here, instead of iterative training, the PW coefficients are optimized. Note that $Z_{k,NL}^\varphi$ in (12) consists the composite higher order basis functions of PAs with negligible power content [6]. Therefore, the optimization aims to minimize the first term of (12) as described later in this section. Next, we describe the proposed two PW schemes.

A. Post-Weighting

The inputs to the PW block are the basis functions of the trained DPD with their nonzero coefficients. For instance, in Fig. 1, there are four basis functions. But, the PW coefficients are multiplied by nonlinear basis functions ($\in \Psi'(s_k, c_k)$) for the required processing. Further, the PW block can vary the value of the coefficients to assign its optimal value. Lastly, the block output is inputted to the PAs to get the desired signals.

1) *Fully-Featured (FF) PW (FF-PW)*: In general, if there are Q nonzero coefficients, $\phi_{kp_1}^{v_1}, \dots, \phi_{kp_Q}^{v_Q}$ of the DPD, their respective nonlinear basis functions are represented as $\psi_{p_1}^{v_1} C_k^{v_1}, \dots, \psi_{p_Q}^{v_Q} C_k^{v_Q} \in \Psi'(s_k, c_k)$. Here, $C_k^{v_i} = \delta(v_i) + c_k \delta(v_i - 1) + c_k^* \delta(v_i - 2)$, $p_i \in \{0, \dots, (P-1)/2\}$ and $v_i \in \{0, 1, 2\}$ such that $p_i \neq 0$ for $v_i = 0$; $i \in \{1, \dots, Q\}$. Because, $\phi_{k0}^0 \phi_{k0}^0 = \phi_{k0}^0 s_k$ for $p_i = 0$ and $v_i = 0$, is the linear component of the input signal to the PW block and is not multiplied by any PW coefficient. $\delta(\cdot)$ is the Kronecker delta function. For instance, in Fig. 1, the DPD has $Q = 3$ nonlinear basis functions. In a subarray, a single DPD linearizes the BO output, but, it is not able to linearize all the PAs due to approximately S times less than required number of coefficients as described in Section I. Therefore, there are nonlinear radiation in different directions. To minimize this, we propose a fully-featured PW scheme as shown in Fig. 1 by solid lines. Here,

different sets of Q PW coefficients are multiplied by nonlinear basis functions for different PAs. Thus, it compensates the required number of coefficients in the DPD to completely linearize the S PAs. The total PW coefficients (or multipliers), $N_\gamma^F = S \times Q$. Also, the total number of adders is $N_a^F = S \times Q$. Therefore, along the Q nonlinear basis functions of the DPD, FF-PW completely do the PW processing for the S PAs. Because, it has $S \times Q$ degree of freedom (or multipliers) to minimize the radiation. In Fig. 1, $Q = 3$ and $S = 4$, and total PW coefficients are 12. The coefficients can be represented as: $\gamma_{klp_1}^{q_1}, \dots, \gamma_{klp_Q}^{q_Q}$; $l \in \{1, \dots, S\}$, $k \in \{1, \dots, K\}$. And, in a vector form, the coefficients are arranged as: $\gamma_k = [\gamma_{k1p_1}^{q_1}, \dots, \gamma_{kSp_1}^{q_1}, \dots, \gamma_{k1p_Q}^{q_Q}, \dots, \gamma_{kSp_Q}^{q_Q}]^T$. As the first term in (12) has the nonlinear basis functions, $\Psi'(s_k, c_k)$, to multiply γ_k with it, we need to rearrange $\Psi'(s_k, c_k)$ along with other matrices and vectors accordingly. So, \bar{h}_k^φ , $\bar{\mathbf{W}}_k$, $\bar{\phi}_{k0}^0$, $\Psi'(s_k, c_k)$, and Φ'_k are arranged as \bar{h}_k^φ , $\bar{\mathbf{W}}_k$, $\bar{\phi}_{k0}^0$, $\bar{\Psi}'(s_k, c_k)$, and $\bar{\Phi}'_k$, respectively. $\bar{h}_k^\varphi = \mathbf{1}_Q \otimes \bar{h}_k^\varphi$, $\bar{\mathbf{W}}_k = \text{diag}(\mathbf{1}_Q \otimes \mathbf{w}_k)$, $\bar{\phi}_{k0}^0 = \text{diag}(\mathbf{1}_Q \otimes \bar{\phi}_{k0}^0)$, $\bar{\Psi}'(s_k, c_k) = \text{diag}(\Psi'(s_k, c_k)^T \otimes \mathbf{1}_S)$, and $\bar{\Phi}'_k = \text{diag}(\Phi'_k \otimes \mathbf{1}_S)$. Now, (12) can be expressed as:

$$\bar{z}_{k,NL}^\varphi = T_k^\varphi \gamma_k + Z_{k,NL}^\varphi, \quad (13)$$

where $T_k^\varphi = \bar{h}_k^\varphi T \bar{\mathbf{W}}_k \bar{\phi}_{k0}^0 \bar{\Psi}'(s_k, c_k) \bar{\Phi}'_k$. As described earlier, due to small power content in $Z_{k,NL}^\varphi$, we neglect the PW effect on it. Moreover, FF-PW provides the best PW optimization performance due to highest degree of freedom. However, it needs large number of multipliers and adders. Also, the required number of RF chains $N_{RF}^F = S$ which is same as the number of PAs. Therefore, to reduce them, we propose a LC-PW scheme.

2) *Low-Complexity Post-Weighting*: In this scheme, we vary the number of PW coefficients according to power content in the nonlinear basis functions of the DPD. In Fig. 1, the LC-PW block and respective connections are represented by dash-dot lines. Here, first, we arrange the Q basis functions from the least order to the higher one or in decreasing order of their power content. Then, for the number of PAs, $S = t^\chi$; $\chi \in \mathbb{P}$, $t \in \mathbb{P} \setminus \{1\}$, $\mathbb{P} = \{1, 2, \dots\}$, we decrease the number of PW coefficients along the basis functions assigned to S PAs in geometric sequence as: $\{S r^\nu, S r^{(\nu+1)}, \dots\}$. $r = t^{-1}$ (< 1) and $\nu \in \mathbb{Z}^+ = \{0, 1, \dots\}$. For example, in Fig. 1, $t = 2$, $\chi = 2$, $\nu = 1$, and $Q = 3$, thus, $S = 4$ and $r = 1/2$. The number of coefficients assigned along the first and second basis functions are: $S r^\nu = 4 \times (1/2)^1 = 2$ and $S r^{(\nu+1)} = 4 \times (1/2)^2 = 1$. But, along the third basis, we assign one coefficient, because, the number cannot be the fractional value, $S r^{(\nu+2)} = 4 \times (1/2)^3 = 1/2$. Therefore, we keep decreasing the number of coefficients when $S r^i \geq 1$; $i \in \{\nu, \nu + 1, \dots, \nu + Q - 1\}$, beyond that we assign one coefficient along each of the remaining basis functions. Thus, in general, the total number of coefficients (or degree of freedom), N_γ^L in the LC-PW is given by (14a) and the total number of adders, N_a^L is expressed in (14b).

$$N_\gamma^L = \begin{cases} S \times \frac{r^\nu(1-r^Q)}{1-r}; & \text{for } S \times r^{(Q+\nu-1)} \geq 1 \\ S \times \frac{r^\nu(1-r^m)}{1-r} + Q - m; & \text{for } \{S \times r^{(m+\nu-1)} \geq 1\} \wedge \{S \times r^{(m+\nu)} < 1\}, \end{cases} \quad (14a)$$

$$N_a^L = N_\gamma^L + S r^\nu - \delta(S r^\nu - Q). \quad (14b)$$

For the first case in (14a), the PW coefficient vector,

$$\gamma_k = [\gamma_{k1p_1}^{v_1}, \gamma_{k(1+r-\nu)p_1}^{v_1}, \dots, \gamma_{k(1+(S-1)r-\nu)p_1}^{v_1}, \dots, \gamma_{k1p_Q}^{v_Q}, \gamma_{k(1+r-(\nu+Q-1))p_Q}^{v_Q}, \dots, \gamma_{k(1+(S-1)r-(\nu+Q-1))p_Q}^{v_Q}]^T \quad \text{and}$$

$$\bar{\Phi}'_k = \text{diag}(\Phi'_k \otimes \mathbf{1}_S) \text{diag}(\underbrace{\mathbf{1}_{r-\nu}, \dots, \mathbf{1}_{r-\nu}}_{S r^\nu \text{ times}}, \dots, \underbrace{\mathbf{1}_{r-(\nu+Q-1)}, \dots, \mathbf{1}_{r-(\nu+Q-1)}}_{S r^{(\nu+Q-1)} \text{ times}}).$$

$$\gamma_k = [\gamma_{k1p_1}^{v_1}, \gamma_{k(1+r-\nu)p_1}^{v_1}, \dots, \gamma_{k(1+(S-1)r-\nu)p_1}^{v_1}, \dots, \gamma_{k1p_m}^{v_m}, \gamma_{k(1+r-(\nu+m-1))p_m}^{v_m}, \dots, \gamma_{k(1+(S-1)r-(\nu+m-1))p_m}^{v_m}, \gamma_{k1p_{(m+1)}}^{v_{(m+1)}}, \gamma_{k1p_{(m+2)}}^{v_{(m+2)}}, \dots, \gamma_{k1p_Q}^{v_Q}]^T \quad \text{and}$$

$$\bar{\Phi}'_k = \text{diag}(\Phi'_k \otimes \mathbf{1}_S) \text{diag}(\underbrace{\mathbf{1}_{r-\nu}, \dots, \mathbf{1}_{r-\nu}}_{S r^\nu \text{ times}}, \dots, \underbrace{\mathbf{1}_{r-(\nu+m-1)}, \dots, \mathbf{1}_{r-(\nu+m-1)}}_{S r^{(\nu+m-1)} \text{ times}}, \dots, \underbrace{\mathbf{1}_S, \dots, \mathbf{1}_S}_{Q-m \text{ times}}).$$

Moreover, remaining vectors and matrices, \bar{h}_k^φ , $\bar{\mathbf{W}}_k$, and $\bar{\phi}_{k0}^0$, $\bar{\Psi}'(s_k, c_k)$ are expressed same as for FF-PW (cf. Section III-A1). Also, the expression for the nonlinear radiation, $\bar{z}_{k,NL}^\varphi$ is same as in (13). Moreover, from Fig. 1, the number N_{RF} of the required RF chains (denoted by dash-dot lines) depends on the number of coefficients applied to first nonlinear basis function, i.e., $N_{RF}^H = S r^\nu = N_{RF}^F r^\nu$.

Thus, in LC-PW, the number of RF chains, multipliers, and the adders are reduced by the factors, $r^{-\nu}$, N_γ^F / N_γ^L , and N_a^F / N_a^L , respectively. For example, in Fig. 1, the respective factors are 2, 4, and 2.4. Hence, the LC-PW is less complex and economical for the mMIMO transmitter.

B. Optimization of γ_k

The optimization problem can be formulated as:

$$\mathcal{P}_0: \text{minimize}_{\gamma_k} \sum_t \mathbb{E}[|\bar{z}_{k,NL}^\varphi|^2]$$

$$\text{s. t. } \bar{h}_k^{\varphi_0 T} \bar{\mathbf{W}}_k \bar{\phi}_{k0}^0 \bar{\Psi}' \bar{\Phi}'_k \gamma_k = \bar{h}_k^{\varphi_0 T} \bar{\mathbf{W}}_k \bar{\phi}_{k0}^0 \bar{\Psi}' \bar{\Phi}'_k \bar{\gamma}_k,$$

where $\bar{\Phi}'_k = \Phi'_k \otimes \mathbf{1}_S$ and $\mathbb{E}[\cdot]$ is the expectation with respect to time samples. In problem \mathcal{P}_0 , the objective function which needs to be minimized in γ_k , is the sum of the average value of the power of nonlinear radiation in the given range of directions with sample points $\{\varphi_t\}$. The constraint ensures the linearization of BO signal in the desired direction φ_0 .

1) *Optimal Solution*: To investigate the convexity of the problem, the objective function, $\mathcal{O}_{\mathcal{P}_0} \triangleq \sum_t \mathbb{E}[|\bar{z}_{k,NL}^\varphi|^2] = \sum_t \mathbb{E}[\bar{z}_{k,NL}^{\varphi_t H} \bar{z}_{k,NL}^{\varphi_t}]$, can be expressed using (13) as:

$$\mathcal{O}_{\mathcal{P}_0} = \gamma_k^H \sum_t \mathbb{E}[T_k^{\varphi_t H} T_k^{\varphi_t}] \gamma_k + \gamma_k^H \sum_t \mathbb{E}[T_k^{\varphi_t H} Z_{k,NL}^{\varphi_t}] + \sum_t \mathbb{E}[Z_{k,NL}^{\varphi_t H} T_k^{\varphi_t}] \gamma_k + \sum_t \mathbb{E}[Z_{k,NL}^{\varphi_t H} Z_{k,NL}^{\varphi_t}]. \quad (15)$$

As the constraint is linear and from (15), the objective function is quadratic in γ_k , the problem, \mathcal{P}_0 is convex and provides a globally optimal solution using the KKT conditions [8]. From \mathcal{P}_0 , the Lagrangian function, $\mathcal{L}(\gamma_k, \eta)$ can be expressed as:

$$\mathcal{L}(\gamma_k, \eta) = \mathcal{O}_{\mathcal{P}_0} + \eta (T_k^{\varphi_0} \gamma_k - \bar{h}_k^{\varphi_0 T} \bar{\mathbf{W}}_k \bar{\phi}_{k0}^0 \bar{\Psi}' \bar{\Phi}'_k \bar{\gamma}_k), \quad (16)$$

where η is the Lagrangian multiplier which is $\neq 0$ to consider the constraint in the optimization. Using the complex gradient of $\mathcal{L}(\gamma_k, \eta)$ in γ_k , the KKT conditions are obtained as:

$$\sum_t \mathbb{E}[T_k^{\varphi_t H} T_k^{\varphi_t}] \gamma_k + \sum_t \mathbb{E}[T_k^{\varphi_t H} Z_{k,NL}^{\varphi_t}] + \eta T_k^{\varphi_0 H} = 0, \quad (17a)$$

$$T_k^{\varphi_0} \gamma_k = T_k^{\varphi_0'}, \quad (17b)$$

where $T_k^{\varphi_0'} = \bar{\mathbf{h}}_k^{\varphi_0 T} \bar{\mathbf{W}}_k \bar{\phi}_{k0}^{-1} \bar{\Psi}^T \bar{\Phi}''_k$. Using (17), the optimal solution, $\hat{\gamma}_k$ and corresponding Lagrangian multiplier, $\hat{\eta}$ are obtained as:

$$\hat{\gamma}_k = \hat{\eta} \left(\sum_t \mathbb{E}[T_k^{\varphi_t H} T_k^{\varphi_t}] \right)^{-1} T_k^{\varphi_0 H} - \left(\sum_t \mathbb{E}[T_k^{\varphi_t H} T_k^{\varphi_t}] \right)^{-1} \times \sum_t \mathbb{E}[T_k^{\varphi_t H} Z_{k,NL}^{\varphi_t}], \quad (18a)$$

$$\hat{\eta} = \frac{T_k^{\varphi_0'} + T_k^{\varphi_0} \left(\sum_t \mathbb{E}[T_k^{\varphi_t H} T_k^{\varphi_t}] \right)^{-1} \sum_t \mathbb{E}[T_k^{\varphi_t H} Z_{k,NL}^{\varphi_t}]}{T_k^{\varphi_0} \left(\sum_t \mathbb{E}[T_k^{\varphi_t H} T_k^{\varphi_t}] \right)^{-1} T_k^{\varphi_0 H}}. \quad (18b)$$

Next, we perform the numerical experiment and describe the various insights on the obtained results.

IV. NUMERICAL EXPERIMENT AND CONCLUSION

To evaluate the performance of the proposed schemes, we use the set of 16 PA memoryless polynomial models obtained by measuring the output of HMC943APM5E PA ICs at 28.5 GHz [9] to the OFDM input signal of 200 MHz bandwidth. Besides, we consider two subarrays, each consists of 16 PAs which are acquired from the same set of PAs. The PAs are arranged in a uniform linear array and the distance between the two antennas is five times the operating wavelength. The beamforming and steering weight for a given azimuth angle is determined using the procedure in [10]. At each antenna, we consider -10 dB crosstalk with random phases. Using the measured output of HMC943APM5E PA ICs at 28.5 GHz with -10 dB crosstalk, we identified the dual-input memoryless model for each PA using LS estimation as follows. For a given input signal $\hat{\mathbf{x}}_k$, a test crosstalk signal $\hat{\mathbf{c}}_{kl}$ to the PA, and the measured output $\hat{\mathbf{y}}_{kl}$, the coefficients of the PA are identified using LS estimation as: $\hat{\mathbf{\Phi}}_{kl} = \mathbf{\Psi}(\hat{\mathbf{x}}_k, \hat{\mathbf{c}}_{kl})^\dagger \hat{\mathbf{y}}_{kl}$. Here, the boldface of the symbols, $\hat{\mathbf{x}}_k$ and $\hat{\mathbf{y}}_{kl}$ represents the signals with their time samples.

Fig. 3 shows the power of nonlinear radiations in different azimuth directions from the transmitters using various PW schemes. They are compared with the radiation power from the transmitter without BO-DPD linearization. We observe a notch in each of the curve at angle, 0 rad, because, BO-DPD linearizes the main lobe directed towards 0 rad. In Fig. 3(a), the PW coefficients are optimized for the angle over the range $\in [-\pi/3, \pi/3]$ where BO-DPD is employed with crosstalk compensation (CTC). Therefore, the radiations overshoots beyond the range from the transmitters using intra and inter PW schemes as described in [6]. But, the proposed schemes perform better in almost all azimuth directions. Considering intra scheme as a benchmark, on average, the inter scheme provides the marginal improvement by 3.44 dB, whereas, LC-PW with $\nu = 1$, $r = 1/2$ and FF-PW schemes give enhancement by 9.88 dB, and 21.01 dB, respectively. Note that the LC-PW performs better than the existing schemes in [6], because, it is addressing the nonlinearities with higher degree of freedom as described in Section III-A2. Moreover, the results in Fig. 3(b) are obtained by optimizing the coefficients for angle over the range $[-\pi/2, \pi/2]$. Here, we compare the PW schemes with and without CTC. The scheme, LC-PW: $\nu = 1$ reduces the nonlinear power by 30.29 dB even without CTC and with CTC, the power is reduced by 33.35 dB. Further, the FF-PW outperforms the other schemes in both scenarios.

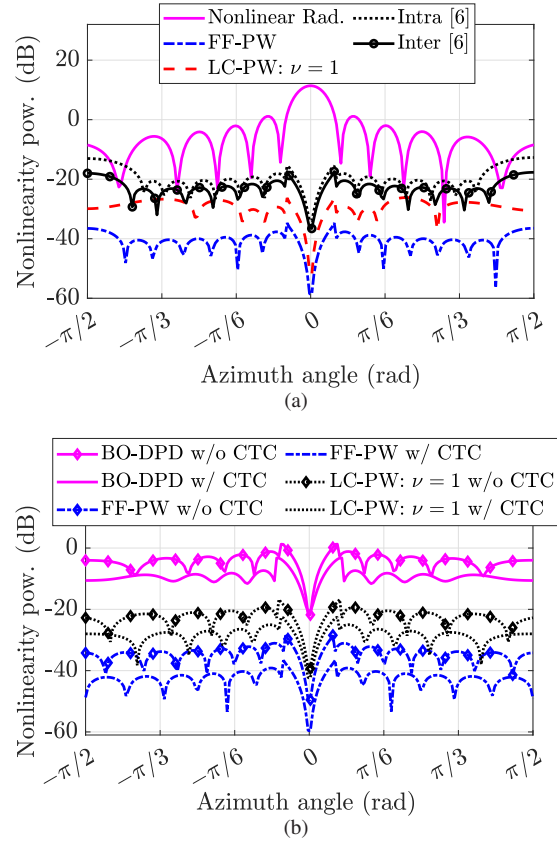


Fig. 3. Performance comparison of the proposed PW schemes against (a) the benchmark schemes and (b) the systems with only BO-DPD.

REFERENCES

- [1] S. A. Bassam, M. Helaoui, and F. M. Ghannouchi, "Crossover digital predistorter for the compensation of crosstalk and nonlinearity in MIMO transmitters," *IEEE Trans. Microw. Theory Tech.*, vol. 57, no. 5, pp. 1119–1128, May 2009.
- [2] Q. Luo, X.-W. Zhu, C. Yu, and W. Hong, "Single-receiver over-the-air digital predistortion for massive MIMO transmitters with antenna crosstalk," *IEEE Trans. Microw. Theory Tech.*, vol. 68, no. 1, pp. 301–315, Jan. 2019.
- [3] M. Abdelaziz, L. Anttila, A. Brihuega, F. Tufvesson, and M. Valkama, "Digital predistortion for hybrid MIMO transmitters," *IEEE J. Sel. Topics Signal Process.*, vol. 12, no. 3, pp. 445–454, Jun. 2018.
- [4] C. Yu, J. Jing, H. Shao, Z. H. Jiang, P. Yan, X.-W. Zhu, W. Hong, and A. Zhu, "Full-angle digital predistortion of 5G millimeter-wave massive MIMO transmitters," *IEEE Trans. Microw. Theory Tech.*, vol. 67, no. 7, pp. 2847–2860, Jul. 2019.
- [5] E. Ng, Y. Beltagy, P. Mitran, and S. Boumaiza, "Single-input single-output digital predistortion of power amplifier arrays in millimeter wave RF beamforming transmitters," in *Proc. IEEE Int. Microw. Symp.-IMS*, Philadelphia, PA, USA, Jun. 2018, pp. 481–484.
- [6] J. Yan, H. Wang, and J. Shen, "Novel post-weighting digital predistortion structures for hybrid beamforming systems," *IEEE Commun. Lett.*, vol. 25, no. 12, pp. 3980–3984, Dec. 2021.
- [7] K. Hausmair, P. N. Landin, U. Gustavsson, C. Fager, and T. Eriksson, "Digital predistortion for multi-antenna transmitters affected by antenna crosstalk," *IEEE Trans. Microw. Theory Tech.*, vol. 66, no. 3, pp. 1524–1535, Mar. 2018.
- [8] S. Boyd, S. P. Boyd, and L. Vandenberghe, *Convex optimization*. Cambridge university press, 2004.
- [9] A. Brihuega, L. Anttila, M. Abdelaziz, T. Eriksson, F. Tufvesson, and M. Valkama, "Digital predistortion for multiuser hybrid MIMO at mmwaves," *IEEE Trans. Signal Process.*, vol. 68, May 2020.
- [10] B. Khan, N. Tervo, M. Jokinen, A. Pärssinen, and M. Juntti, "Statistical digital predistortion of 5G millimeter-wave RF beamforming transmitter under random amplitude variations," *IEEE Trans. Microw. Theory Tech.*, vol. 70, no. 9, pp. 4284–4296, Sep. 2022.